A PREDICTION OF WELDING PROCESS CONTROL VARIABLES BY PREDICTION OF WELD BEAD GEOMETRY USING FACTORIAL DESIGN APPROACH

S. THIRUCHITRAMBALAM
S. HEMAVATHI
SUNIL PANDEY

UNIVERSITI TEKNIKAL MALAYSIA MELAKA

A PREDICTION OF WELDING PROCESS CONTROL VARIABLES BY PREDICTION OF WELD BEAD GEOMETRY USING FACTORIAL DESIGN APPROACH

S.Thiruchitrambalam[1,a*], S.Hemavathi[2,b] and Sunil Pandey[3,c]

[1] Universiti Teknikal Malaysia Melaka (UTeM), Melaka, Malaysia
*[a]E-mail: thiru@utem.edu.my,
[2]School of Civil Engineering, Linton University College, Negeri Sembilan, Malaysia.
[b]Email:hema@legendagroup.edu.my
[3]Department of Mechanical Engineering, Indian Institute of Technology Delhi (IITD), India.
[c]Email: spandey@mech.iitd.ac.in

Abstract— Plasma Enhanced Shielded Metal Arc Welding (PESMAW) is a modified version of the age old manual metal arc welding (MMA) where the cellulose based flux coated solid wires are replaced by tubular low hydrogen flux coated electrodes. PESMAW process is aimed to eliminate the usage of cellulose in the electrode coating so as to save some trees and hence make the welding process partially green. The high heat content of the cellulose supported arc is achieved by controlled supply of auxiliary plasma gas through the tubular wire directed into the arc. This paper discusses the influence of the welding process parameters to the weld bead characteristics of weldments made by PESMAW process using mild steel as base metal. Two level fractional factorial design was adopted to investigate and quantify the direct and interactive effects of four major control parameters. "Bead on plate" technique was used to lay weldments and bead geometry was measured using standard metallurgical procedures. Statistical models were made from the obtained results and were analyzed and tested by using analysis of variance technique and students't' test. The estimated and obtained values were compared. The main and interactive effects of control parameters were studied and presented in graphical form.

Keywords—Weld bead geometry, Design of Experiments, Fractional Factorial Design

I. INTRODUCTION

For open root pass girth welding, manual welding with cellulosic electrodes is still the most widely applied process in spite of the increasingly becoming popular GMAW and GTAW processes [1,2]. Welds made by Cellulosic electrodes, are highly susceptible to hydrogen induced cold cracking (HICC), an invisible, hard to predict and yet a "could be lethal" weld defect infamously responsible for some of the most catastrophic yet spectacular failures recorded in the welded structure history. The pipeline industry however has learnt to live with this defect with "inbuilt" expenses viz., pre-heating, post-heating, and 100% radiographic testing of root welds as the cellulosic electrodes generate a forceful arc, producing high penetration welds- a mandatory requirement for pipe welding. This makes the industry to cope with the kind of defects it potentially inherits from using cellulosic electrodes, not with standing the huge losses it incurs from production delays and sporadic fatal failures [3].

However attempts have been made by researchers to develop alternative methods to reduce the hydrogen levels in girth welds. The plasma enhanced shielded metal arc welding (PESMAW) [4], a variant of shielded metal arc welding, is one among these attempts, aimed to amplify the penetration levels of general purpose rutile coated electrodes at comparatively lower currents so as to make it usable for making pipe welds. This paper presents an investigation made on weldment characteristics such as penetration with respect to the most important process control variables viz., varying arc current, welding speed, orifice gas flow rate and electrode angle.

A. PESMAW process

The plasma enhanced Shielded metal Arc welding (PESMAW) is a method of welding, cutting, piercing and surfacing metals, with an electric arc and a stream of selective gases or gas mixtures (CO_2, O_2 Ar, He, Ar + CO_2 mixture). Equipment includes a specially designed Universal Electrode Holder (UEH) which houses provisions for holding tubular covered electrodes and gas supply, an A.C. or D.C. welding machine, gas tank and regulating gauges. The PESMAW electrode is a ferrous metal tube covered with a low hydrogen coating. The function of the tubular electrode, which is consumed during operation, is to conduct current for the establishment and maintenance of the arc. The bore of the tube directs the auxiliary plasma gas to the metal being welded. Both current and gasses are fed to the electrode through the holder.

In PESMAW process, welding begins when an arc is struck between the tip of the electrode and the work. The high intensity arc melts the tip of the tubular covered electrode as well as the surface of the work below. Tiny globules of molten metal start flowing from the molten tip of the electrode due to the arc force. The orifice gas when introduced at the middle of the arc gets ionized instantaneously due to the high arc temperature. This ionized gas produces a number of effects. First, it increases the heat input rate of the arc and hence the arc energy by increasing the weld pool temperature. Second,

the gas broadens the arc, makes the heat input distribution broader. This will change the surface tension gradients on the weld pool and thereby alter fluid flow. Finally, the centreline velocity of the orifice gas accelerates the flow of molten metal globules that increases the strength of the plasma jet thereby depress the centre of the weld pool further which results in deeper penetration [5].

II. EXPERIMENT

A. Experimental configuration

The experimental configuration consisted of a specially built semi automatic welding system, welding machine, gas tanks and the tubular covered electrode fitted to the Universal Electrode Holder (UEH), a specially designed welding torch, which houses provisions for holding electrodes and gas supply for performing the PESMAW process. The semi automatic welding system is built in such a way that the UEH with consumable-coated electrode, could be set at any required angle with in 180 degrees to the work piece by fastening it to an insulated block. The block, in turn was attached to a lead screw whose angular velocity could be varied by a variable speed stepper motor, thus provided the means for altering the arc travel rate of the electrode. This stepper motor unit was placed over a carriage, which could be moved vertically up and down, was attached to a lead screw and was driven by a frequency controlled variable speed motor for altering the down feed in order to make the desired arc length. Both the travel speed and down feed were calibrated before its use. Output lines from the power source were connected to the table and electrode respectively.

Since the unit design precluded "striking" an arc as is done manually, another method was devised to ignite the arc. After positioning the test piece on the carriage plate, the electrode was set at a sizable distance above its surface. The power source, carriage and electrode motions were then started simultaneously. When the electrode reached an optimum distance for arc initiation, a sharp edged copper-coated graphite rod was inserted manually to ignite the arc. Once the electrode down feed was adjusted to provide a reasonably constant arc length, the welding operation was continued. Table-1 gives the welding conditions used for the current study.

TABLE 1. Welding parameters and their limits.

Parameter	Unit	Limits	
		Low (-1)	High (+1)
Welding current (I)	A	90	110
Arc travel rate (S)	mm/min	120	240
Orifice gas flow rate (G)	lit/min	0	1.25
Electrode angle (θ)	degree	60	90

B. Experimental method

Cold rolled mild steel plates of 6.5x50x150 mm were used as base metal and the weld specimens were prepared by applying linear "bead on plate" technique. The specimens were cleaned chemically and mechanically to remove the oxide layer and any other source of hydrogen prior to welding. All welding were carried out using rutile coated AWS E6013 (High Titania Potassium) electrodes. The diameter of the electrode tube was 3.25 mm with an inner diameter of 1.6mm. All electrodes measured 355 mm long with a coating ratio of 1.58. The nominal composition of the electrode is given in Table 1.

TABLE 2. Chemical composition of base metal.

C	Si	Mn	S	P	Ni
0.179	0.140	0.466	0.029	0.047	0.005
Cr	Cu	Zr	Ti	Nb	Co
0.042	0.155	0.01	0.011	0.010	0.001

A 6.3-kVA constant current, high frequency microprocessor controlled, portable inverter SMAW/TIG welding power source, was used for the experiments. A specially designed manually operated welding torch, which uses tubular covered electrodes instead of solid electrodes and requires an external source of gas supply for performing the Plasma Enhanced Shielded Metal Arc Welding (PESMAW) process was made. The electrode has three sections: the torch body, the gas entry chamber and the electrode tip assembly. The torch body is also the handle. It utilizes the straight slot collet for gripping the electrode that is screwed on to the end of the torch. Multiple collets are used for different electrode diameters.

III. FACTORIAL DESIGN APPROACH FOR MATHEMATICAL MODELLING

Factorial designs are widely used in experiments where all the factors in the experiment are varied at their respective levels simultaneously to investigate the joint effects, typically the main effects and low order interactions of the factors on a response variable. An interaction can be thought of as a new factor, which is a combination of two or more factors. Interactions are not intuitive and their effects are hard to predict. A factorial experiment can be either full factorial or fractional factorial. A full factorial design of experiment is generally represented by 2^k, (k is the number of factors) where all factor settings are chosen such that all possible combinations are tested. But as the number of factors (k) is increased, the number of required trials (2^k) is also increased geometrically. Since, geometrically increased number of trials is mainly due to estimate the increased number of higher order interactions, which in most of the cases do not affect the response significantly [6]. The matrix can still be very large and therefore, trials for conducting for such estimates may not suitable for a variety of reasons including lack of necessary materials, lack of time available on the machine, lack of man-hours, or all of the above.

To perform DOE studies without a full factorial matrix, statisticians have devised fractional factorial matrices where a certain set or combinations are not tested by

using the concept of confounding; the reduced set of experiments is called a fractional-factorial. A fractional factorial experiment is generally represented by (2^{k-p}), where $1/(2^p)$ represents the fraction. In the fractional factorial designed experiment, the main effects of the factors are mixed (confounded) with the effects of higher order interactions. Since, these higher order interaction effects are assumed to be statistically insignificant, therefore, resulting estimates are essentially the estimates of the main effects.

IV. PREDICTION OF THE BEAD GEOMETRY ACCORDING OT FRATIONAL FACTORIAL APPROACH

A. Selection of Design

The welding variables were identified with a view to developing mathematical models to predict the two important characteristics of weld bead geometry viz., the weld penetration and weld reinforcement. Since the PESMAW process is fundamentally a variant of the manual metal arc welding process, the selection of two main variables such as the welding current and welding speed that directly govern the weld bead geometry was made from the wide literature available for the conventional arc welding processes [7-9]. However since the PESMAW process uses orifice gas to generate supplementary plasma, the gas flow rate (G) and the angle at which the gas is introduced in to the weld pool (θ) were identified as the other two defining variables to control weld metal characteristics. A two-level half-factorial design was selected to get complete insight into the main and interaction effects of the parameters on weld bead geometry. The reasons for selecting two level factorial design to conduct the experiments are following:

- From the results of most of the earlier studies [7], it was found that the functional relationships between various welding parameters involved in coated stick electrodes were fundamentally linear.
- The range, covering the low and the high level of the direct welding parameters involved in this experiment was small.
- The two level factorial design helped in reducing the experimental runs to the minimum possible, which in turn reduced the total experimental time.

As in the present investigation, four independently controllable variables were involved so two- level full factorial design would require $2^4 = 16$ runs for each set of the experiments. However, the two- level half-fractional factorial design of eight (2^{4-1}) runs was selected and the effect of all the four variables were investigated simultaneously by confounding the main effects with three parameters interactions. A set of eight runs were repeated twice to test the significance and adequacy of the models. The same design, welding parameters range, design matrix, model and procedure were used to develop the models for bead geometry.

B. Selection of the model Development of a design matrix

The response function Y, representing the bead geometry parameters, can be represented as:

$$Y = f(I, G, S, \theta) \qquad (1)$$

where the responses variable, 'Y' could be any of the bead geometry and shape relationship (BG&SR) responses viz. penetration (p), bead width (w), crown height (h) etc. The direct process parameters I, G, S and θ represents the welding current, orifice gas flow rate, welding speed and electrode angle respectively. Assuming a linear relationship in the first instant and taking into account all the possible two factor interactions, the above expression can be expressed as:

$$Y = b_0 + b_1 I + b_2 G + b_3 S + b_4 \theta + b_{12} IS \\ + b_{13} IG + b_{14} I\theta + b_{23} SG + b_{24} S\theta + b_{34} G\theta \qquad (2)$$

Where, b_0, b_1, b_2 ... b_{34} are the coefficients of the polynomial equation.

C. Development of the Design Matrix

Factorial design can be represented in the form of design matrix where column and row correspond to levels of the factors and the different experimental runs respectively. The sign of the columns of design matrix were selected according to the limits shown in Table 1 and in such a way that these are having certain necessary optimal properties viz., a) symmetry relative to the centre of experiment b) normalization c) orthogonality and d) rotatability such that after confounding of the interaction effects and neglecting the higher (more than two) order interaction effects, the design matrix can be represented as per Table 3 and model can be represented as follows:

TABLE 3. The Design matrix.

S.No	Direct parameters			
	I	S	G	θ
1.	+	+	+	+
2.	-	+	+	-
3.	+	-	+	-
4.	-	-	+	+
5.	+	+	-	-
6.	-	+	-	+
7.	+	-	-	+
8.	-	-	-	-

$$Y = b_0 + b_1 I + b_2 G + b_3 S + b_4 \theta + b_5 (IS + G\theta) \\ + b_6 (IG + S\theta) + b_7 (I\theta + SG) \qquad (3)$$

Where,

$$b_5 = b_{12} + b_{34}; \qquad b_6 = b_{13} + b_{24}; \qquad b_7 = b_{14} + b_{23}$$

Thus, on the assumption that the three parameters and higher order interactions were negligible, the fractional design (two- level half factorial) of eight runs provided eight estimates for the effects of four parameters. One estimate is for the mean effect of all the parameters, four estimates are for the main effects of each factor and three estimates are for the two factor interaction effects.

D. Cochran's Test for Homogeneity of Variances

Before the regression analysis homogeneity of the variances is to be tested .The homogeneity of variances implies that there are no variances among the ones being summated and considerable exceeds the remaining ones. The homogeneity of the variances can be tested by applying Cochran's criterion. It is confirmed homogenous if the experimental value of G, which is the ratio of the maximum variances to the sum of all the variances:

$$G = \frac{S_{max}^2}{\sum\limits_{i=1}^{N} s_i^2} \quad (4)$$

Where, 'G' and S_{max}^2 are the experimental value of Cochran's criterion and maximum variance respectively.

E. Evaluation of the Coefficients

The coefficients of the selected model were calculated using the method of least squares as per equation 5.

$$b_j = \frac{\sum\limits_{i=1}^{N} X_{ji} Y_i}{N}, j = 0,1...,k \quad (5)$$

Where, X_{ji}, Y_i, N and k are the value of the factor or interaction in the coded form, average value of the response parameters, number of observation and number of trials of the model respectively.

F. Significance of the Coefficients

The statistical significance of the coefficients of the model can be tested by applying 't' test to eliminate the insignificant coefficients. The extent of significance of a particular parameter can be assessed by the magnitude of the 't' value associated with it. Higher the value of 't', the more significant it becomes. Coefficients having calculated 't' values less than or equal to 't' value from the standard table for eight degree of freedom and 95% confidence level, are the members of reference distribution i.e. they could be merely due to the intrinsic variations of the experimentation and hence, they were insignificant. The value of 't' from the standard table for eight degree of freedom and 95% confidence level is 2.3. The significance of each coefficients is determined separately by applying 't'. The calculated 't' value of each coefficient is compared with the tabulated 't' value. If the calculated 't' is more than that of the tabulated 't' value, then the coefficient is considered to be significant. Variance of optimization can be given as:

$$S_y^2 = 2\frac{\sum\limits_{o=1}^{N}(Y_{ol} - Y_{avg})^2}{N} = 2\frac{(\Delta Y)^2}{N} = \frac{\sum\limits_{i=1}^{N} S_i^2}{N} \quad (6)$$

Where,
Y_{Ol} is the one of the observed values of the two responses,
Y_{avg} is the average value of the two response,
N is the degree of freedom = number of trials,
S_i^2 is the variance of a response,

ΔY is the sum of all the variances $= \sum\limits_{i=1}^{N} S_i^2$

The calculated 't' value can be obtained as $t = \frac{|b_j|}{S_{bj}}$

Where,

$|b_j|$ is the absolute value of the coefficient,

S_{bj} is the standard deviation of the coefficient $= \sqrt{\frac{S_y^2}{N}}$

G. Adequacy of the Model

The adequacy of the model was determined by the analysis of variance technique .The variance of the response and 'F'-ratio of the model were calculated as per method given below. The 'F'-ratio of the model is the ratio of the variance of adequacy to the variance of optimization parameter:

$$F_{Model} = \frac{S_{ad}^2}{S_y^2} \quad (7)$$

The 'F'-ratio of the developed model was compared with the tabulated value of 'F', obtained from the standard table. If the calculated value of F-ratio is less than that of tabulated value, then the model is considered adequate. In the present study, tabulated 'F' value for 95% confidence interval at 3 degree of freedom of the variance of adequacy and 8 degree of freedom of variance of optimization respectively is 4.1. Variance of adequacy can be expressed as:

$$S_{ad}^2 = \frac{\sum\limits_{o=1}^{N}(Y_{o3} - Y_{Est})^2}{d.f} \quad (8)$$

Where,
Y_{O3} is the third observed values of the response,
Y_{Est} is the estimated value of the two response,
$d.f.$ is the degree of freedom $= N-(k+1)$,
'k' is the number of independent variables.

V. THE RELATIONSHIP BETWEEN BEAD PARAMETERS AND WELDING PROCESS PARAMETERS

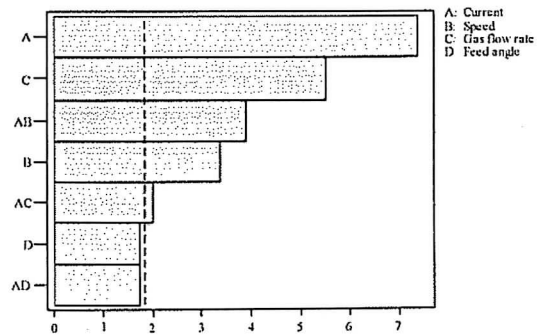### A. Developed model for Bead Penetration (p)

Figure 1   Pareto plot of the main and interaction effects on weld penetration (p)

The developed model for the prediction of weld penetration after dropping the statistically insignificant coefficients, in the coded form is:

$$p = 1.47 + 0.17I - 0.08S + 0.13G - 0.09IS \quad (9)$$

The Pareto chart Fig 1 clearly indicates the significant process parameters that affect the weld penetration. The sensitivity of the model is demonstrated from the scatter diagram plotted between the estimated values through the mathematical model and observed values (Fig 2).
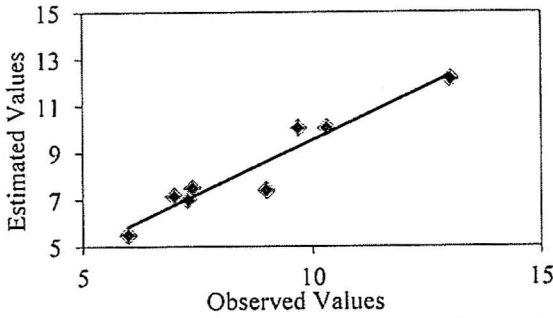

Figure 2. Scatter diagram between the estimated and observed values of weld penetration (p)

B. Main and Interactive Effects

Welding current, speed and the auxiliary gas flow rate were the parameters that showed statistically significant main effect on the weld penetration. Welding current along with speed also showed statistically significant interaction effect on weld penetration. The direct relationship between the weld penetration to the determining parameters is shown in Figs 3, 4 and 5. Fig 6 shows the effect on weld penetration of the interaction of welding current and welding speed. Response surface due to the interaction of two selected parameters is shown in Fig 7.
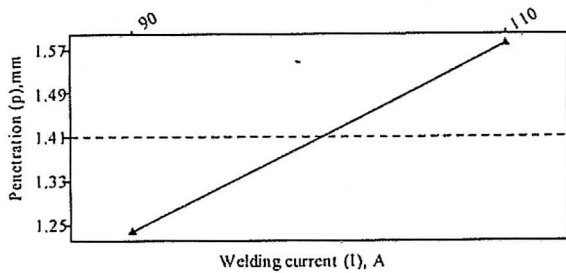

Figure 3   Effect of welding current (I) on weld penetration (p)

It is clearly observed from the model that the weld penetration increases with an increase in current. As shown in Fig 3, the penetration increases from 1.30 to 1.64 mm with the increase in welding current from 90A to 110A. The higher arc energy due to the raised current is the cause for this expansion. It is attributed to the increase in digging power [4] of the arc due to the increase in the welding current density. Consequently the current intensity of the arc amplifies, which in turn accumulates the digging power of the arc and hence penetration.

However, penetration is found to be in decreasing trend with an increase in weld speed- Fig 4, and at lower current levels the weld speed appeared to have much lesser influence on penetration – Fig 5. From the former, it is clearly shown that an increase in welding speed from 120 mm/min to 240 mm/min reduces the penetration level from 1.55mm to 1.39mm, which means the increasing trend of the penetration decreases with the increase in welding speed. The decrease in heat input, metal deposition rate and digging power of the arc due to the increase in welding speed are the possible reasons for this phenomenon. At higher current levels however, due to the high deposition rate, more liquid metal accumulates under the arc leaving substantial area of base metal unexposed to the digging arc which results in less penetration.
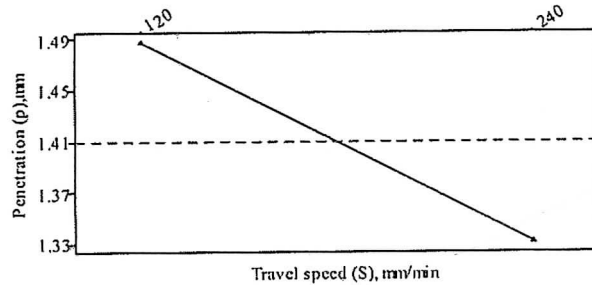

Figure 4   Effect of welding speed (S) on weld penetration (p)

However, at low current level there was no such drastic reduction in penetration was observed with respect to the welding speed. In fact there was a slight increase in penetration found from low to high speed which could be attributable to the low melting rate due to low current. All these outcomes are very much analogous to the published results of the conventional arc welding processes [10, 11].
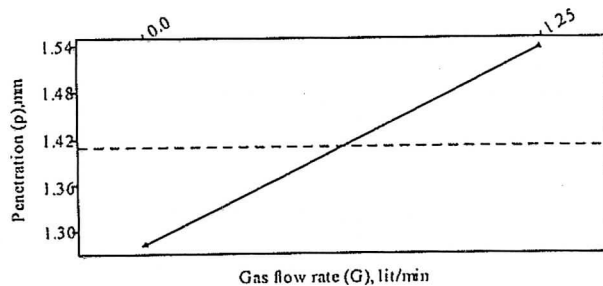

Figure 5   Effect of Gas flow rate (G) on weld penetration (p)

The influence of orifice gas flow on weld penetration was distinctly demonstrated from Fig 5 as there was a substantial increase in depth of penetration during gas flow.The orifice gas flow has proven to be one of the main determining factors in generating increased penetration levels, which understandably shows the significance of PESMAW process over the conventional SMAW process. The improved penetration levels observed in CO_2 gas fed tubular electrodes in PESMAW gives proof for plasma generation [4] at the tip of the electrode.
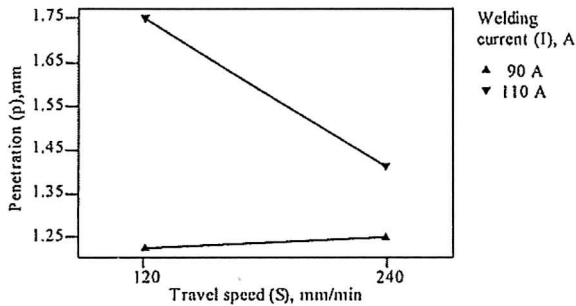

Figure 6   Interaction effect of welding speed (S) and current (I) on weld penetration (p)

The gas fed into the weldment would constitute fully ionized plasma due to the peak temperature at the middle of the arc, which increases the heat of the arc coupled with high centerline velocity, accelerates the detached droplets, results in improved penetration.
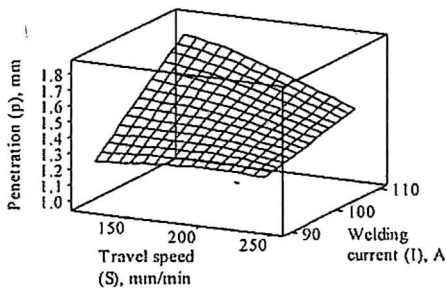

Figure 7   Response surface due to interaction of welding speed (S) and current (I) with weld penetration (p)

VI. CONCLUSIONS

1. The two level factorial techniques could be effectively employed for developing statistical models for predicting the weld-bead geometry and shape factors within the design limit of the parameters. The observed and estimated values of weld penetration (p) was found to have good correlation within the designed limit of the parameters.

2. The welding current (I), arc travel rate (S), auxiliary gas flow rate (G) and electrode feed angle (θ) influenced the bead geometry and shape relationship significantly within the designed limits.

3. Weld penetration (p), was found to be increasing with increasing welding current (I), and auxiliary gas flow rate (G). However, increase in welding speed resulted in decrease in penetration of the weld bead. It was also found that the interaction effect of weld current (I), and the arc travel rate (S) were found to affect penetration significantly.

REFERENCES

[1]   M.P.Jain, Welding & NDT of oil & gas pipelines-productivity & quality issues, *National seminar on cost effective welding & productivity, Indian welding society (IWS)*, New Delhi, India, 2002, 115.

[2]   A.C. Underwood, Automated welding will meet the desperate need for more pipelines in the United States, *Welding Design & Fabrication*, November 1980, 134-135.

[3]   R. L. Klien, *Pipelines Design, construction and operation*.2, New York, Construction press, 1984, 3-4.

[4]   Sunil Pandey, New Technologies in Shielded metal Arc welding and Gas Metal Arc Welding. *National Welding Seminar, Indian Institute of Welding (IIW)*, Chennai, India, 2002.

[5]   Sunil Pandey, Tahir I. Khan, S.Thiruchitrambalam, Surface modification of steels using plasma enhanced shielded metal arc welding process (PESMAW), *Indian welding journal*, April 2003, 27-30.

[6]   Box George E.P.,Hunter William G.,Stuart Hunter J.,*Statistics for experimenters An introduction to design, Data analysis and model building*, John Willey & sons, 1978, pp. 653-659.

[7]   Nagesh D. S.,Datta G. L.,Prediction of weld bead geometry and penetration in shielded metal-arc welding using artificial neural networks, *Journal of Materials Processing Technology*, April 2002, pp. 303-312

[8]   Lee J. I.,Um K. W.,A prediction of welding process parameters by prediction of back-bead geometry, *Journal of Materials Processing Technology*, Dec. 2000, pp. 106-113.

[9]   Chandel R.S.,Orr R.F., Effect of process variables on bead geometry of the submerged arc strip overlay welds, *Indian Welding Journal*, Jan. 1984, pp. 21-29.

[10]   McGlone J.C., Weld bead geometry prediction- a review, *Metal Construction*, July 1982, pp. 378-384.

[11]   Ravichandran G.,Buvanasekaran G.,Mohankumar V.,Raju A.S.,Effect of process variables on dilution and bead geometry in single strip stainless steel cladding, *Proceedings of National welding seminar*, Tiruchirappalli, India, 1983, pp. 15.1-15.11.